Macrophages at low-inflammatory status improved osteogenesis *via* autophagy regulation

Lan Yang [1,2,#], Lan Xiao[2,3,#], Wendong Gao[1,2], Xin Huang[2], Fei Wei[2], Qing Zhang[1], Yin Xiao[1,2,3,*]

[1] Key Laboratory of Oral Medicine, Guangzhou Institute of Oral Disease, Stomatology Hospital of Guangzhou Medical University, Guangzhou, China

[2] Institute of Health and Biomedical Innovation, Queensland University of Technology, 60 Musk Avenue, Kelvin Grove, Brisbane, QLD 4059, Australia

[3] The Australia-China Centre for Tissue Engineering and Regenerative Medicine (ACCTERM)

[#] Those authors contributed equally to this paper.

* Correspondence: Prof Yin Xiao (PhD), yin.xiao@qut.edu.au; Tel.: +61-7 31386240

Contact information for other authors:

Lan Yang (DDS): yangl1900@163.com, +61 0469812246

Lan Xiao (DDS, PhD): l5.xiao@qut.edu.au, +61-7-31386099

Wendong Gao (PhD): w22.gao@qut.edu.au, +61 0405846678

Xin Huang (DDS): x35.huang@hdr.qut.edu.au, +61-7-31380214

Fei Wei (PhD): f2.wei@hdr.qut.edu.au, +61 0448127677

Qing Zhang (Master): qzbuct@126.com, +86 17316150369

Abstract: Accumulating evidence indicates that the interaction between immune and skeletal systems is vital in bone homeostasis. However, the detailed mechanisms between macrophage polarization and osteogenic differentiation of mesenchymal stromal cells (BMSCs) remain largely unknown. We observed enhanced macrophage infiltration along with bone formation *in vivo*, which showed a transition from early stage M1 phenotype to later stage M2 phenotype, cells at the transitional stage expressed both M1 and M2 markers actively participated in osteogenesis, which was mimicked by stimulating macrophages with lower inflammatory stimulus (as compared with typical M1). Using conditioned medium (CM) from M0, typical M1, low-inflammatory M1 (M1^{semi}), and M2 macrophages, it was found that BMSCs treated with M1^{semi} CM showed significantly induced migration, osteogenic differentiation, and mineralization, compared to others. Along with the induced osteogenesis, the autophagy level was the highest in M1^{semi} CM treated BMSCs, which was responsible for BMSC migration and osteogenic differentiation, as autophagy-interruption significantly abolished this effect. This study indicated that low-inflammatory macrophage could activate autophagy in BMSCs to improve osteogenesis.

Keywords: Osteoimmunology, Macrophage, Autophagy, Osteogenesis, Bone, Regeneration

Impact Statement: The interaction between macrophage polarization and osteogenic differentiation of mesenchymal stromal cells (BMSCs) plays a decisive role in bone homeostasis, whereas the detailed mechanisms remain largely unknown. In this study, we found macrophage at low-inflammatory status (M1semi), which expressed both M1 and M2 markers was actively involved in osteogenesis, which induced the migration, osteogenic differentiation and mineralization of BMSCs, as compared with M0, M1 and M2 macrophages, which was partially achieved by activating autophagy in BMSCs. This study identified low-inflammatory macrophage, as the transitional macrophage during M1-to-M2 switch in bone formation, could activate autophagy in BMSCs to improve osteogenesis.

1. Introduction

Treatment of large bone defects due to trauma, cancer, infectious bone loss and developmental congenital disorders remains a very difficult and challenged clinical problem, especially for the healing of bone non-union, which affects patients' health and well-being and thereby causing severe social and financial problems. Bone is a dynamic tissue with life-long remodeling, a process consists of bone resorption and formation,[1] suggesting bone is a self-healable tissue at suitable circumstances. Thereby, to achieve functional regeneration in large bone defects, the ultimate solution is to understand the mechanisms governing bone formation.

Bone formation is a process initiated by bone marrow derived stromal cells (BMSCs) differentiating into osteoblasts.[2, 3] Recent studies have found that the interactions between immune and skeleton systems, termed as "osteoimmunology",[4] act as decisive regulators for bone remodeling regulation.[5-7] Macrophages have been identified as key modulators in bone forming process *via* interaction with BMSCs.[8] As one of the major cells types in the innate immune system, macrophages are a group of plastic cells with multiple phenotypes. The non-activated M0 macrophages polarize towards a spectrum of phenotypes under different stimuli, and the two ends of this spectrum are termed as pro-inflammatory M1 (classically activated by lipopolysaccharide (LPS) and interferon γ (IFNγ)) and tissue-regenerative M2 (alternatively activated by interleukin 4 (IL-4) and IL-13).[9-17] Macrophage polarization plays crucial regulatory roles in bone regeneration, that M1 macrophages take dominance at the early stage of bone healing, while as the healing process goes on, the M1 macrophages are gradually converted into M2 macrophages.[18-20] Biomaterials inducing the M1 to M2 conversion have been demonstrated to promote bone regeneration, suggesting M2 macrophages would benefit osteogenesis, as M2-derived factors such as bone morphogenetic protein-2 (BMP-2) and TGF-β promote osteogenic differentiation and mineralization.[21-23] However, it is also widely recognized that the early stage inflammatory macrophage infiltration is indispensable in bone fracture healing.[24, 25] Recent findings demonstrated that in comparison with M2 macrophages, M1 (inflammatory) macrophages also showed osteo-inductive effects, which secreted pro-inflammatory cytokine IL-6 to induce osteogenesis *via* the oncostatin M (OSM)-STAT3

signaling pathway.[19, 26] Interestingly, bone morphogenetic protein 2 (BMP-2), a clinical used cytokine for bone repair has been found to induce an inflammatory-like phenotype in macrophages.[27] Thereby, the detailed roles of macrophage polarization spectrum on bone regeneration are still not fully understood.

The interaction between macrophages and BMSCs is achieved through cytokines, receptors and signaling pathways.[6] Among these, autophagy plays elementary roles in both immune[28] and skeletal[29] systems. Autophagy is a highly conserved "self-eating" lysosomal degradation process in eukaryotic cells, which facilitates intracellular waste clearance and maintains cell homeostasis.[30, 31] Previous studies have shown that autophagy is induced during osteogenic differentiation, and autophagosome functions as cargoes to transport the intracellular mineral crystals to extracellular matrix (ECM), an indispensable part in bio-mineralization and bone regeneration.[32] Autophagy gene deletion *in vivo* resulted in decreased bone formation while induced production of receptor activator of nuclear factor kappa B ligand (RANKL)[32] to facilitate the differentiation of bone resorbing osteoclasts.[33, 34] As macrophage-BMSC interaction is indispensable in bone regeneration, it is therefore speculated whether macrophage regulates the autophagy level during osteogenesis. Hence, the present study aimed to investigate the effects of macrophage phenotype spectrum on osteogenic differentiation, and to detect whether autophagy was involved in the macrophage-BMSC interaction in bone formation.

2. Materials and Methods

Animal study

All experimental procedures conformed to the Guiding Principles of the Ethics Committee of Queensland University of Technology, Australia (ethics approval number: 1300000144), and Stomatology Hospital of Guangzhou Medical University, China (ethics approval number: 20190325001). Fifteen 6 week-old male Wistar rats were used for subcutaneous osteogenesis model induction following the published protocol.[35] Briefly, after shaving and disinfecting the dorsal skin, two incisions sized at 4-5 mm were created along the central dorsal surface of rat under anesthesia. 50 mg collagen was gently mixed with 100 μL saline

and 16 µL recombinant human BMP-2 (rhBMP-2, 500 µg/mL, Shanghai Rebone Biomaterials Co.). Collagen (at the same amount) mixed with 116 µL saline served as the control. Each rat received subcutaneous implantation of collagen (control group) on the left-hand side, and collagen with BMP-2 (BMP-2 group) on the right-hand side. Five rats were sacrificed at 1, 4, 7 days after surgery, to harvest the subcutaneous tissues around implants. These samples were fixed with 4% paraformaldehyde (PFA) for 24 h at room temperature, and then demineralized in 10 % EDTA solution for 4 weeks. After dehydration, these samples were embedded in paraffin, and then cut into 5-µm sections.

H&E staining

To investigate general morphology, the sections were stained with haematoxylin and eosin following the previous publication.[36] One in every four sections was collected and analyzed by using a Leica slide scanner (Leica Microsystems, Wetzlar, Germany) and analyzed with Image J software to count the total cell number of the image, which was performed in a double-blind manner. For each sample, five randomly chosen sections were used to calculate the average cell counting number.

Immunohistochemistry

Immunohistochemical (IHC) staining was performed as previously described[36] to detect the expression of CD68, iNOS, arginase and beclin 1 in the subcutaneous samples at different time points. Rabbit polyclonal antibodies against CD68 (1:300), iNOS (1:100), arginase (1:200) and beclin 1 (1:200) (Abcam, Cambridge, UK) were used (were diluted in PBS containing 0.1% BSA) as primary antibodies. After three-times washing with PBS, sections were incubated with EnVision™+ Dual Link System-HRP for 30 min (secondary antibodies). Images were captured using a Leica slide scanner, and analyzed by Image J software to measure the positive-stained cells in a double-blind manner. Five sections from each sample were analyzed for cell measurements.

Double immunofluorescence labelling

IF (IHC) staining was performed as previously described[36] to detect the macrophage transition (CD86$^+$CD206$^+$ cells) in the subcutaneous samples (4 d). Rabbit polyclonal

antibodies against CD206 (1:200) and CD86 (1:100) (Abcam, Cambridge, UK) were used simultaneously (diluted in PBS containing 0.1% BSA) as primary antibodies. Goat anti-rabbit Alexa Fluor® 488 and goat anti-mouse Alexa Fluor® 568 (1:500, Cell Signaling Technology) secondary antibody were used. All antibodies were diluted in 0.1% bovine serum albumin (BSA). Results were analyzed with Nikon A1R Confocal Microscope (Nikon, Minato, Tokyo, Japan). All experiments were replicated for three times.

Cell culture

BMSCs were obtained from 8-10-week-old Wistar male rats (rBMSCs) as described previously.[37] Cells within 5 passages were used for experiments. For *in vitro* osteogenic differentiation, cells were treated with osteogenic medium (10 mM β-glycerophosphate, 50 μM ascorbic acid and 100 nM dexamethasone in DMEM with 10 % fetal bovine serum (FBS) and 1% penicillin/streptomycin (P/S)). Spautin-1 (5 or 10 ng/ml, Sigma-Aldrich Pty Ltd) or rapamycin (0.05 or 0.1 ng/ml, Sigma-Aldrich Pty Ltd) was added into osteogenic medium to interrupt[38] or promote[39] autophagy in rBMSCs during osteogenesis, respectively. The cells with DMSO or equal volume of PBS served as controls. Cells were harvested on 7/14days of differentiation for subsequent experiments.

To study the macrophage-BMSC interaction, RAW 264.7 (RAW) cells was used, which were cultured in DMEM with 5 % FBS (heat-inactivated at 60 °C for over 30 min) and 1% P/S (culture medium was changed every 2 days).

***In vitro* rBMSC and RAW cell interaction model**

For macrophage polarization stimulation, RAW cells were treated with PBS (M0), IFN-γ (100 ng/ml) and LPS (10 ng/ml for M1[semi], or 100 ng/ml for typical M1) or IL-4 (100ng/ml, M2) for 12 h, washed twice with phosphate-buffered saline (PBS), then starved with serum-free DMEM for another 12 h to harvest the conditioned medium (CM).[26, 40] RAW cells were harvested. The CM was subjected to centrifugation (1000×g, 10 min, 4 °C) then filtered with a 0.45-μm filter (Millipore Corporation, Billerica, MA, USA), and stored at -80 °C for further experiments.

To investigate the effects of M0/M1semi/M1/M2 macrophages on osteogenesis, the CM was mixed (1:1) with two-times osteogenic medium (DMEM, 20 % FBS, 2 % P/S, 20 mM β-glycerophosphate, 100 µM ascorbic acid and 200 nM dexamethasone), and the mixture was used to treat rBMSCs.[26] Spautin-1 (10 ng/ml) or rapamycin (0.05 ng/ml) was added into M1semi CM to interrupt autophagy in rBMSCs. After differentiation for 3/7/14 days, rBMSCs were harvested accordingly for subsequent experiments.

MTT assay

The MTT assay was used to evaluate the effects of CM, spautin-1 and rapamycin on the proliferation of rBMSCs as previously described.[41] Briefly, rBMSCs were seeded into 96-well plates (2,000 cells/well, three wells/group) and treated with CM, spautin-1 (0, 2, 4, 8 or 10 ng/ml) or rapamycin (0, 0.02, 0.04, 0.08, 0.1 ng/ml) in DMEM supplemented with 10% FBS and 1% P/S. After 1, 2, 3, 4, 5 or 7 days, the culture medium was removed, 100 µl fresh culture medium (DMEM with 10% FBS) containing MTT solution (0.5 mg/mL, Sigma-Aldrich Pty Ltd) was added to each well and incubated at 37°C for 4 h. After medium removal, 100 µl dimethyl sulfoxide (DMSO) was added into each well to solubilize the formazan product. The absorbance was read at 490 nm by a plate reader (Molecular Devices, LLC, San Jose, CA). All experiments were repeated for three times.

Transwell assay

To detect the effect of macrophage CM on migration of rBMSCs, transwell assay was performed. Briefly, rBMSCs (20,000 cells/insert, 3 inserts/group) were seeded onto 8.0 µm-transwell inserts (BectonDickinson Labware, Franklin Lakes, NJ, USA). CM was deposited in the lower chambers with DMEM as control. Spautin-1 (10 ng/ml) or rapamycin (0.05 ng/ml) was added into M1semi CM to interrupt or improve autophagy in rBMSCs, respectively. After 8 h, cells in the upper chamber were removed, and cells migrated to the other side of the membrane were fixed with 4% PFA and stained with 1% crystal violet solution. Images were taken with light microscope (Eclipse TS100, Nikon Australia Pty Ltd.) and analysed by Image J software. For migration quantification, cell numbers of 5 randomly selected fields/sample were measured, and three separated assays were performed).

RNA extraction, cDNA synthesis, and real time quantitative-PCR (qPCR)

Total RNA was extracted from RAW cells or rBMSCs (3/7 days of differentiation) using the TRIzol Reagent (Ambion®, Thermo Fisher Scientific, Waltham, MA, USA). 1 μg total RNA was used to synthesize cDNA by using the SensiFAST™ cDNA Synthesis Kit (Bioline Reagents, Meridian Bioscience Inc., Cincinnati, OH, USA). QPCR was performed to analyse the mRNA levels of the following genes: *iNOS, CD86, CCR7, OSM, CD11c, IL-1a, IL-1b, IL-6, TNF, Arg-1, CD206, CD163, BMP2, TGF-β, Wnt5a,* and *Wnt10b* (RAW cells); *Runx2, OCN, OPN, ALP, Smad1, Smad4, Smad5, BMPR2, VEGF, VEGFR, ATG5, ATG7 and Beclin 1* (rBMSCs). The house-keeping genes *Gapdh* and *Actb* were used as controls. Primer sequences were listed in Table 1 and Table 2 in Supplemental material. Relative gene expression was normalized against *Gapdh* or *Actb* and calculated as previously described.[42] All experiments were following the MIQE guidelines[43] and replicated for three times.

Protein extraction and western blotting

Total protein was extracted from rBMSCs (7 days of differentiation) using lysis buffer (20 mM HEPES (pH 7.4), 10% glycerol, 1% Triton X-100, and 2 mM EDTA) containing cOmplete™ protease inhibitor cocktail (Roche, Dee Why, NSW, Australia). Protein concentration of the extracts was measured by using the BCA Protein Assay Kit (Thermo Fisher Scientific) following the manufacturer's protocol. Western blotting was performed as previously described.[40] Primary antibodies (rabbit-originated) against ALP (1:1000, Abcam, Cambridge, UK), Col-1 (1:500, Abcam) and LC3 A/B (1:1000, Cell Signaling Technology, Danvers, MA) were used (antibody against α-Tubulin (1:2000, Abcam) was used as loading control). The anti-rabbit IgG IRDye 800 conjugated secondary antibody (1:10000, Rockland, Gilbertsville) was used as secondary antibody. The membranes were then scanned and analysed using an Odyssey® Infrared Imaging System and Image Studio software (LI-COR Biosciences) according to the manufacturer's instructions. All antibodies were diluted in Odyssey Blocking Buffer. All procedures were replicated for three times.

Alizarin Red S staining

After 14 days of osteogenic differentiation, rBMSCs were fixed with 4 % PFA. The cells were washed with ultra-pure water, and then stained with 1% Alizarin Red S solution (pH: 4.1-4.3, Sigma-Aldrich Pty Ltd) for 20 min at room temperature. After washing with ultra-pure water, the samples were imaged with a stereoscopic microscope. Three separated assays were performed.

Scanning electron microscopy

After 14 days of osteogenic differentiation, rBMSCs were fixed with 3% glutaraldehyde overnight, then rinsed three times with 0.1M cacodylate. After post-fixed with 4% osmium for 1 h, the samples were sequentially dehydrated with graded (50%, 70%, 90%, 90%, 100% and 100%, 10-15 min/each). After coated with platinum-palladium sputtering, the samples were then examined under Zeiss Scanning electron microscopy (SEM) (FEI, USA).

Statistical analysis

Student's t-tests were performed for comparison between two groups. Comparison between multiple groups were performed with statistical analysis using one-way ANOVA followed by the Student-Newman-Keul test at $\alpha = 0.05$ using Prism 7.0 (Graphpad software, California, USA). $p < 0.05$ was considered as significantly different.

3. Results

Induced macrophage infiltration and polarization in subcutaneous osteogenic model

As shown in Figure 1, BMP-2 group showed obvious bone-like tissues in 7 days after implantation (as indicated by arrows), whereas in the control group only fibrous tissues could be found. There were more cells condensed in the implantation site in BMP-2 group, as further confirmed by cell counting (Figure 1B). The cell types generally consisted of fibroblast-like cells and infiltrating immune cells (Figure 1A).

To detect macrophage infiltration, immunohistochemistry (IHC) staining against CD68 was performed. The percentage of CD68-positive cells kept increasing from day 4 to day 7 in

BMP-2 group (Figure 2A), whereas, for the control group, CD68-positve cells could merely be observed with a significantly lower population (Figure 2B). To determine the polarization of these macrophages, iNOS-positive cells (M1-like) and arginase-positive (M2-like) cells were detected in BMP-2 group, and the percentages of these cells were significantly higher than those in the control group at each time point (Figure 2B). It was also noted that the percentage of iNOS-positive cells peaked on day 4 and decreased thereafter, whereas the percentage of arginase-positive cells increased from day 4 to day 7.

M1 to M2 transition during bone formation *in vivo*

Double-immunofluorescent (IF) staining was performed to label cells expressing both M1 (CD86) and M2 (CD206) markers.[44] Figure 3 showed the CD86+ cells (red) and CD206+ cells (green) cells in day 4 samples. CD86 and CD206 double-positive cells could be observed clearly in BMP-2 group, indicating the M1 to M2 transition during bone formation *in vivo*. This phenomenon was scarcely observed in later stage (day 7) at BMP-2 group, as well as in both day 4 and day 7 samples from the control group (Figure 3) . These results evidenced the transition phase of M1 to M2 in the early osteogenesis.

Macrophages with low-level of inflammatory stimulation improved osteogenesis

In vitro experiments were performed to investigate the interaction of macrophage polarization spectrum with BMSCs during osteogenesis. As macrophages gradually loss the M1 phenotype during M1 to M2 transition, in this study, macrophages semi-stimulated with much lower doses of inflammatory stimulus than the typical M1 were used to compare the effects of transitional M1 and typical M1 on osteogenesis. As shown in Figure 4A, the typical (M1 group) and lower-inflammatory M1 (M1^semi group) phenotypes were characterized, which all showed induced inflammatory markers (CCR7, CD86, iNOS, IL-1α/β) as compared with M0. Compared with the typical M1, M1^semi showed reduced inflammatory markers (iNOS and IL-1β) while induced tissue-regenerative/osteogenic factors OSM, BMP2 and Wnt10b (Figure 4A).[19, 27, 45] Furthermore, M1^semi CM was found to induce rBMSC mineralization, as compared with the CM from typical M1 (Figure 4B),

suggesting low-inflammatory macrophage would be more beneficial for osteogenesis. Thereby, the M1^{semi} CM was used in the following studies.

The characteristics of M0, M1^{semi} and M2 were then compared. As shown in Figure 4C, the mRNA levels of inflammatory markers (CCR7, CD11C, CD86, iNOS, IL-1β, IL-6 and TNF) and osteo-inductive marker OSM were found to be significantly enhanced in cells from the M1^{semi} group, as compared with M0 and M2 groups. On the other hand, the mRNA levels of M2 anti-inflammatory markers (Arg-1, CD163, CD206) were significantly induced in M2 group (Figure 4C).

Low-inflammatory macrophages promoted migration, metabolism, and osteogenic differentiation of rBMSCs

The effects of M0, M1^{semi} and M2 CM on rBMSCs were then compared. From the transwell assay results (Figure 5A&B), it could be observed that M1^{semi} CM induced rBMSC migration, as compared with the blank control. Especially, compared with M0 and M2 CM, there were more cells attracted by M1^{semi} CM, as shown in the images (Figure 5A) and the quantification (Figure 5B). MTT assay was performed to investigate the effect of CM on rBMSC metabolism, and the result showed that M1^{semi} CM significantly enhanced the metabolism levels in rBMSCs from day 2 to day 5 (Figure 5C), as compared with the blank control group. No significant differences were found among the control, M0 CM and M2 CM groups.

To find out the effects of macrophages on osteogenesis, M0, M1^{semi} and M2 CM was used to stimulate rBMSCs during osteogenic differentiation. Cells treated by M1^{semi} CM showed significantly elevated mRNA levels of osteogenic markers (ALP, Runx2, OCN, Figure 5D). Smad1/4/5, BMPR2, VEGF and VEGFR were also up-regulated in M1^{semi} CM-treated cells (Figure 5D). Accordingly, the protein levels of ALP and Col-I increased in M1^{semi} CM-treated cells (Figure 5E). On 14 days of osteogenic differentiation, enhanced mineralization[46] could be observed in the M1^{semi} CM group (Figure S1A). The M0 and M2 CM-treated groups also showed stronger stain than the control group (Figure S1A). SEM was performed to observe the structure of mineralization, which showed that unlike the other three groups with

mineralized "dots" with cells, the mineralization of M1^{semi} CM-treated group appeared as large aggregated minerals (Figure S1B).

Autophagy was induced during bone formation *in vivo*, as well as in rBMSCs treated by CM from low-inflammatory macrophages

To detect autophagy, IHC staining was performed to label beclin 1-positive cells, which showed that beclin 1 was significantly induced in BMP-2 group as compared with the control (Figure 6A). Similar to iNOS (Figure 2B), beclin 1 expression reached the peak on day 4, and then decreased on day 7 in BMP-2 group. (Figure 5A).

To find out whether autophagy was involved in M1^{semi} CM-directed osteo-inductivity, autophagy level was examined in osteogenic differentiation cells. As shown in Figure 6B, M1^{semi} CM treated cells showed significantly induced ATG5 and ATG7 at 3 and 7 days of differentiation, as compared with the control group. Although beclin 1 expression in M1^{semi} CM was lower on day 3, it was significantly much higher than the control group on day 7 (Figure 6B). No increase of these autophagy-related genes could be found in M0 CM group when compared with the control. In M2 CM group, induced ATG5 and beclin 1 were also found as compared with the control group (Figure 6B). Moreover, the WB result showed that in M1^{semi} CM group, the LC3-II protein level was significantly higher than the other three groups, accordingly, the LC3-II to LC3-I ratio was also the highest in M1^{semi} CM group (Figure 6C).

Low-inflammatory macrophages promoted migration and osteogenesis in an autophagy-dependent manner

To verify whether autophagy was related with M1^{semi} CM-directed osteogenesis, autophagy level was modulated in rBMSCs. Autophagy-inhibitor (spautin-1) and activator (rapamycin) were used, and the effects were tested in rBMSCs during osteogenic differentiation. MTT result (Figure 6D) showed that both spautin-1 and rapamycin down-regulated cell metabolism. The WB result showed that rapamycin induced LC3-II level and spautin-1 reduced LC3-II level dose-dependently, respectively (Figure 6E). Along with LC3-II change, ALP was induced or reduced (Figure 6E), respectively. Rapamycin (0.05 ng/ml) enhanced matrix mineralization[46] and spautin-1 (10 ng/ml) inhibite mineralization[46] (Figure

6F). Thereby, spautin-1 at 10 ng/ml was chosen to interrupt autophagy in M1^{semi} CM-directed cells. As shown in Figure 7A, with spautin-1, the cell migration was significantly reduced in comparison with M1^{semi} CM group.Meanwhile, osteogenic gene markers (OCN, OPN and Runx2) were down-regulated on both day 3 and day 7 in spautin-1 treated cells (Figure 7B). The protein levels of LC3-II and ALP were also down-regulated in M1^{semi} CM-treated cells with spautin-1 treatment (Figure 7C). The mineralization was reduced accordingly (Figure 7D).

4. Discussion

In the present study, a subcutaneous osteogenic model by BMP-2 implantation was established to investigate the macrophage-BMSC interaction. BMP-2, a clinical used cytokine with demonstrated bone regenerative effect,[27] successfully formed subcutaneous bone-like structures at 7 days after implantation. Along with osteogenesis was the induced cell aggregation. Especially, the positive correlation between macrophage infiltration and bone formation suggests the crucial role of macrophage in bone formation. There was a trend of transition from M1-like to M2-like macrophages in the osteogenic environment. This timely transition was in accordance with the previous findings that M1 to M2 switch is considered as a key part in bone regeneration.[18-20] Especially, the identification of cells with both M1 (CD86) and M2 (CD206) markers was confirmed in the early osteogenic environment induced by BMP-2, which further supporting the M1 to M2 transition in bone formation. It is worth noting that the osteogenesis model used in the current study is an ectopic model, although it has been accepted as a model for studying bone formation,[47-50] it differs from orthotopic bone regeneration on aspects such as comparably lower cytokine stimulation, mechanical force stimulation and cellular interaction with endogenous osteogenic cells from host bone.[47] Further investigation will be conducted to detect the phenomenon of M1-to-M2 transition in an orthotopic bone formation model in the future study.

Further studies were performed to detect the role of this transition in bone formation. Our previous study has found that a unique macrophage phenotype stimulated by RANKL, with expression of low-inflammatory markers, has higher osteo-inductivity, as compared with

typical M1.[26] This suggested the low-inflammatory macrophages (which appeared during M1 to M2 transition) might be more beneficial for osteogenesis. Thereby, macrophages were induced with high- (typical M1) and low-inflammatory (M1^{semi}) stimulation, and a co-culture model using macrophage CM[26] was applied, to compare their effects on osteogenesis. M1^{semi} macrophage showed lower expression of *IL-1β*, a factor with demonstrated negative effects on osteogenesis at high concentration,[51] while the expression of osteogenic factors–*OSM, BMP-2 and Wnt* 10b[19, 27, 45]–were induced in M1^{semi} macrophage. Accordingly, M1^{semi} CM induced mineralization as compared with typical M1. Thereby, the lower inflammatory macrophage enhanced osteo-inductivity than typical M1.

The osteo-inductive effects of low-inflammatory macrophage were further compared with M0 and M2 by using the similar CM-based co-culture model. RBMSCs treated with CM from low-inflammatory macrophage showed the highest osteogenesis, evidenced by the elevated *BMPR2, VEGF* and *VEGFR*. VEGF is an angiogenesis marker which directs neo-vascular formation by activating its receptor VEGFR,[52] an indispensable part in bone repairing process,[53] which directly improved bone regeneration *in vivo.*[54] Hence, in comparison with M0 and M2, the low-inflammatory macrophage should be more beneficial for osteogenesis.

Our data also indicated elevated autophagy level in early stage of bone formation *in vivo*. To investigate whether autophagy was involved in macrophage-BMSC interaction, three autophagy-related genes were examined in rBMSCs, and the results indicated that a significant increase on autophagy in low-inflammatory macrophage CM treated rBMSCs, which was further confirmed the induced conversion of protein LC3-I to LC3-II–a autophagy hallmark.[55] These results suggested that treatment with low-inflammatory M1 CM not only induced osteogenesis, but also upregulated autophagy in rBMSCs. Especially, when interrupting autophagy level in cells treated with M1^{semi} CM (with spautin-1, as confirmed in reduced LC3-I to LC3-II conversion), the migration and osteogenic differentiation of BMSCs were reduced. Thereby, our findings indicated that low-inflammatory M1 macrophage-directed osteogenesis induction was achieved, at least partially, through autophagy activation on BMSCs.

The phenomenon of M1 to M2 transition has long been observed during bone regeneration, that the dominant M1 gradually loss the inflammatory phenotype along with BMSCs' osteogenic differentiation and eventually transfer into M2 with new bone formation. A recent study suggested that M1 macrophage promoted mineralization of mesenchymal stem cells *via* the COX-2-Prostaglandin E2 pathway,[25] whereas other studies found that the conversion from M1 to M2 macrophages facilitated osteogenesis *in vitro*.[22] Especially, soluble factors from M2 macrophages but not from M0 or M1 macrophages were found to promote mineralization of mesenchymal stem cells *in vitro*; furthermore, M0 and M1 macrophages only promoted early and middle stages of osteogenesis.[23] However, the detailed relationship between this transition and bone regeneration (especially *in vivo*) is not clear yet, especially . In the current study, we observed transitional macrophage-like cells in the midterm of bone formation, which expressed both M1 and M2 markers. Furthermore, we found lower-inflammatory macrophage showed the best osteo-inductivity, as compared with M0, M1 and M2 phenotypes, an effect partially achieved by activating autophagy level in BMSCs. This suggests that macrophages at transitional phase (with lower inflammatory markers and higher osteogenic markers) might play a more important role to facilitate BMSC osteogenic differentiation, as compared with the M1 and M2 phenotypes which are at the two ends of macrophage spectrum. Thereby, the current study potentially unveils the mechanisms underlying the role of M1-M2 transition in bone regeneration.

5. Conclusions

Taken together, our findings demonstrate that in comparison with M0, M1 and M2 phenotypes, macrophages with lower-inflammatory stimulation show better osteogenesis, which activate autophagy in BMSCs to facilitate their migration into the regenerating site, differentiation to osteogenic lineage and bone formation.

Supplementary Material: Supplementary figures and Table 1&2 can be found in Supplementary material.

Author Contributions: Conceptualization, L.Y., L.X and Y.X.; methodology, L.Y., L.X., W.G., X.H., F.W., Q.Z.; formal analysis, L.Y., L.X., Y.X.; resources, Y.X.; data curation, L.Y., L.X.,

W.G., X.H., F.W., Q.Z.; writing—original draft preparation, L.Y., L.X., Y.X.; writing—review and editing, Y.X.; supervision, Y.X.; project administration, L.X.; funding acquisition, Y.X. All authors have read and agreed to the published version of the manuscript.

Conflicts of Interest: The authors declare no conflict of interest.

Reference

1.   Raggatt LJ and Partridge NC. Cellular and molecular mechanisms of bone remodeling. *Journal of Biological Chemistry* 2010; 285: 25103-25108.

2.   Kini U and Nandeesh B. Physiology of bone formation, remodeling, and metabolism. *Radionuclide and hybrid bone imaging*. Springer, 2012, pp.29-57.

3.   Franz-Odendaal TA, Hall BK and Witten PE. Buried alive: how osteoblasts become osteocytes. *Developmental dynamics: an official publication of the American Association of Anatomists* 2006; 235: 176-190.

4.   Dewhirst FE, Stashenko PP, Mole JE, et al. Purification and partial sequence of human osteoclast-activating factor: identity with interleukin 1 beta. *The Journal of Immunology* 1985; 135: 2562-2568.

5.   Arron JR and Choi Y. Osteoimmunology: bone versus immune system. *Nature* 2000; 408: 535-536.

6.   Takayanagi H. Osteoimmunology: shared mechanisms and crosstalk between the immune and bone systems. *Nature Reviews Immunology* 2007; 7: 292-304.

7.   Nauta AJ and Fibbe WE. Immunomodulatory properties of mesenchymal stromal cells. *Blood* 2007; 110: 3499-3506.

8.   Chang MK, Raggatt L-J, Alexander KA, et al. Osteal tissue macrophages are intercalated throughout human and mouse bone lining tissues and regulate osteoblast function in vitro and in vivo. *The Journal of Immunology* 2008; 181: 1232-1244.

9.   Colton CA and Wilcock DM. Assessing activation states in microglia. *CNS & Neurological Disorders-Drug Targets (Formerly Current Drug Targets-CNS & Neurological Disorders)* 2010; 9: 174-191.

10.   Colton CA. Heterogeneity of microglial activation in the innate immune response in the brain. *Journal of neuroimmune pharmacology* 2009; 4: 399-418.

11.	Ponomarev ED, Maresz K, Tan Y, et al. CNS-derived interleukin-4 is essential for the regulation of autoimmune inflammation and induces a state of alternative activation in microglial cells. *Journal of Neuroscience* 2007; 27: 10714-10721.

12.	Yang X, Xu S, Qian Y, et al. Resveratrol regulates microglia M1/M2 polarization via PGC-1α in conditions of neuroinflammatory injury. *Brain, behavior, and immunity* 2017; 64: 162-172.

13.	Hu X, Leak RK, Shi Y, et al. Microglial and macrophage polarization—new prospects for brain repair. *Nature Reviews Neurology* 2015; 11: 56.

14.	Horwood NJ. Macrophage Polarization and Bone Formation: A review. *Clinical reviews in allergy & immunology* 2015: 1-8.

15.	Mantovani A, Sica A, Sozzani S, et al. The chemokine system in diverse forms of macrophage activation and polarization. *Trends in immunology* 2004; 25: 677-686.

16.	Mills CD, Kincaid K, Alt JM, et al. M-1/M-2 macrophages and the Th1/Th2 paradigm. *The Journal of Immunology* 2000; 164: 6166-6173.

17.	Murray PJ, Allen JE, Biswas SK, et al. Macrophage activation and polarization: nomenclature and experimental guidelines. *Immunity* 2014; 41: 14-20.

18.	Loi F, Cordova LA, Zhang R, et al. The effects of immunomodulation by macrophage subsets on osteogenesis in vitro. *Stem Cell Res Ther* 2016; 7: 15. 2016/01/24. DOI: 10.1186/s13287-016-0276-5.

19.	Guihard P, Danger Y, Brounais B, et al. Induction of osteogenesis in mesenchymal stem cells by activated monocytes/macrophages depends on oncostatin M signaling. *Stem Cells* 2012; 30: 762-772. 2012/01/24. DOI: 10.1002/stem.1040.

20.	Xiao L, Zhou Y, Friis T, et al. S1P-S1PR1 Signaling: the "Sphinx" in Osteoimmunology. *Frontiers in Immunology* 2019; 10. Review. DOI: 10.3389/fimmu.2019.01409.

21.	Chen Z, Klein T, Murray RZ, et al. Osteoimmunomodulation for the development of advanced bone biomaterials. *Materials today* 2016; 19: 304-321.

22. Loi F, Córdova LA, Zhang R, et al. The effects of immunomodulation by macrophage subsets on osteogenesis in vitro. *Stem cell research & therapy* 2016; 7: 1-11.

23. Zhang Y, Böse T, Unger RE, et al. Macrophage type modulates osteogenic differentiation of adipose tissue MSCs. *Cell Tissue Res* 2017; 369: 273-286. 2017/04/01. DOI: 10.1007/s00441-017-2598-8.

24. Schlundt C, El Khassawna T, Serra A, et al. Macrophages in bone fracture healing: their essential role in endochondral ossification. *Bone* 2018; 106: 78-89.

25. Lu LY, Loi F, Nathan K, et al. Pro-inflammatory M1 macrophages promote Osteogenesis by mesenchymal stem cells via the COX-2-prostaglandin E2 pathway. *J Orthop Res* 2017; 35: 2378-2385. 2017/03/02. DOI: 10.1002/jor.23553.

26. Huang R, Wang X, Zhou Y, et al. RANKL-induced M1 macrophages are involved in bone formation. *Bone Research*; 5: 17019.

27. Fu R, Selph S, Mcdonagh M, et al. Effectiveness and harms of recombinant human bone morphogenetic protein-2 in spine fusion: a systematic review and meta-analysis. *Annals of Internal Medicine* 2013; 158: 890-902.

28. Deretic V, Saitoh T and Akira S. Autophagy in infection, inflammation and immunity. *Nature Reviews Immunology* 2013; 13: 722-737. DOI: 10.1038/nri3532.

29. Srinivas V, Bohensky J, Zahm AM, et al. Autophagy in mineralizing tissues Microenvironmental perspectives. *Cell Cycle* 2009; 8: 391-393. DOI: DOI 10.4161/cc.8.3.7545.

30. Wong E and Cuervo AM. Integration of Clearance Mechanisms: The Proteasome and Autophagy. *Csh Perspect Biol* 2010; 2. DOI: ARTN a006734

10.1101/cshperspect.a006734.

31. Lee JY, Koga H, Kawaguchi Y, et al. HDAC6 controls autophagosome maturation essential for ubiquitin-selective quality-control autophagy. *The EMBO journal* 2010; 29: 969-980.

32. Nollet M, Santucci-Darmanin S, Breuil V, et al. Autophagy in osteoblasts is involved in mineralization and bone homeostasis. *Autophagy* 2014; 10: 1965-1977.

33. Theill LE, Boyle WJ and Penninger JM. RANK-L and RANK: T cells, bone loss, and mammalian evolution. *Annual review of immunology* 2002; 20: 795-823.

34. Kong Y-Y, Yoshida H, Sarosi I, et al. OPGL is a key regulator of osteoclastogenesis, lymphocyte development and lymph-node organogenesis. *Nature* 1999; 397: 315-323.

35. Gillette R, Mardfin DF and Schour I. Osteogenesis in subcutaneous rib transplants between normal and ia rats. *Developmental Dynamics* 1956; 99: 447-471.

36. Xiao L, Zhou Y, Zhu L, et al. SPHK1-S1PR1-RANKL Axis Regulates the Interactions Between Macrophages and BMSCs in Inflammatory Bone Loss. *J Bone Miner Res* 2018; 33: 1090-1104.

37. Leboy PS, Beresford JN, Devlin C, et al. Dexamethasone induction of osteoblast mRNAs in rat marrow stromal cell cultures. *Journal of cellular physiology* 1991; 146: 370-378.

38. Shao S, Li S, Qin Y, et al. Spautin-1, a novel autophagy inhibitor, enhances imatinib-induced apoptosis in chronic myeloid leukemia. *International Journal of Oncology*; 44: 1661---1668.

39. Takeuchi H, Kondo Y, Fujiwara K, et al. Synergistic augmentation of rapamycin-induced autophagy in malignant glioma cells by phosphatidylinositol 3-kinase/protein kinase B inhibitors. *Cancer Research* 2005; 65: 3336-3346.

40. Xiao L, Wei F, Zhou Y, et al. Dihydrolipoic Acid–Gold Nanoclusters Regulate Microglial Polarization and Have the Potential To Alter Neurogenesis. *Nano Letters* 2020; 20: 478-495. DOI: 10.1021/acs.nanolett.9b04216.

41. Wu C, Zhou Y, Fan W, et al. Hypoxia-mimicking mesoporous bioactive glass scaffolds with controllable cobalt ion release for bone tissue engineering. *Biomaterials* 2012; 33: 2076-2085.

42.   Bookout AL and Mangelsdorf DJ. Quantitative real-time PCR protocol for analysis of nuclear receptor signaling pathways. *Nuclear receptor signaling* 2003; 1.

43.   Bustin SA, Benes V, Garson JA, et al. The MIQE guidelines: minimum information for publication of quantitative real-time PCR experiments. *Clinical chemistry* 2009; 55: 611-622.

44.   Song J, Choi S-M and Kim BC. Adiponectin regulates the polarization and function of microglia via PPAR-γ signaling under amyloid β toxicity. *Frontiers in cellular neuroscience* 2017; 11: 64.

45.   Roser-Page S, Vikulina T, Zayzafoon M, et al. CTLA-4Ig-Induced T Cell Anergy Promotes Wnt-10b Production and Bone Formation in a Mouse Model. *Arthritis & Rheumatology*; 66: 990-999.

46.   Dai Z, Shu Y, Wan C, et al. Effects of culture substrate made of poly (n-isopropylacrylamide-co-acrylic acid) microgels on osteogenic differentiation of mesenchymal stem cells. *Molecules* 2016; 21: 1192.

47.   Scott MA, Levi B, Askarinam A, et al. Brief review of models of ectopic bone formation. *Stem Cells Dev* 2012; 21: 655-667. 2012/01/04. DOI: 10.1089/scd.2011.0517.

48.   Giannoni P, Scaglione S, Daga A, et al. Short-time survival and engraftment of bone marrow stromal cells in an ectopic model of bone regeneration. *Tissue Engineering Part A* 2010; 16: 489-499.

49.   Zhou M, Geng Y-m, Li S-y, et al. Nanocrystalline hydroxyapatite-based scaffold adsorbs and gives sustained release of osteoinductive growth factor and facilitates bone regeneration in mice ectopic model. *Journal of Nanomaterials* 2019; 2019.

50.   Wei F, Liu G, Guo Y, et al. Blood prefabricated hydroxyapatite/tricalcium phosphate induces ectopic vascularized bone formation via modulating the osteoimmune environment. *Biomaterials science* 2018; 6: 2156-2171.

51.   Perrien DS, Brown EC, Fletcher TW, et al. Interleukin-1 and Tumor Necrosis Factor Antagonists Attenuate Ethanol-Induced Inhibition of Bone Formation in a Rat Model of

Distraction Osteogenesis. *Journal of Pharmacology and Experimental Therapeutics* 2002; 303: 904-908. DOI: 10.1124/jpet.102.039636.

52.   Ferrara N, Gerber H-P and LeCouter J. The biology of VEGF and its receptors. *Nature Medicine*; 9: 669-676.

53.   Maes C, Carmeliet P, Moermans K, et al. Impaired angiogenesis and endochondral bone formation in mice lacking the vascular endothelial growth factor isoforms VEGF164 and VEGF188. *Mechanisms of Development* 2002; 111: 61-73.

54.   Zhou Y, Huang R, Fan W, et al. Mesenchymal stromal cells regulate the cell mobility and the immune response during osteogenesis through secretion of vascular endothelial growth factor A. *J Tissue Eng Regen Med* 2018; 12: e566-e578. 2016/10/04. DOI: 10.1002/term.2327.

55.   Tanida I, Ueno T and Kominami E. LC3 and Autophagy. *Methods Mol Biol* 2008; 445: 77-88.

Table 1. Primer sequences for the genes investigated in this study (mouse)

Gene	Full name	Forward sequences	Reverse sequences
CCR7	C-c motif chemokine receptor 7	5'ACTGCCTTCACTCTGCATTTG3'	5'CGTGGTATTCTCGCCGATGT3'
CD11C	Integrin Subunit Alpha X	5'ACTTCACGGCCTCTCTTCC3'	5'CACCAGGGTCTTCAAGTCTG3'
CD86	CD86 antigen	5'CTGCTCATCATTGTATGTCAC3'	5'ACTGCCTTCACTCTGCATTTG3'
TNF	Tumor necrosis factor	5'CTGAACTTCGGGGTGATCGG3'	5'GGCTTGTCACTCGAATTTTGAGA3'
iNOS	Nitric oxide synthase 2, inducible	5'TGGTGAAGGGACTGAGCTGT3'	5'CTGAGAACAGCACAAGGGGT3'
IL-6	Interleukin 6	5'GTCTTCTGGAGTACCATAGCTACCTG3'	5'CCTTCTGTGACTCCAGCTTATCTG3'
IL-1α	Interleukin 1 alpha	5' CTCCAGCTGGAGGAAGTTAAC 3'	5'CTGACTCAAAGCTGGTGGTG3'
IL-1β	Interleukin 1 beta	5' TGG AGA GTG TGG ATC CCA AG3'	5'GGT GCT GAT GTA CCA GTT GG3'

| OSM	Oncostatin M	5'ACGGTCCACTACAACACCAG3'	5'CCATCGTCCCATTCCCTGAAG 3'
Arg-1	Arginase, liver	5'CAGTACAGCAAGGTCCTTGC3'	5'AGGGTCTACGTCTCGCAAGCCA3'
BMP2	Bone morphogenetic protein 2	5'GACACAGTTCCCTACAGGGAG 3'	5'ATGGTCGACCTTTAGGAGAC3'
TGF-β	Transforming growth factor beta 1	5'CAGTACAGCAAGGTCCTTGC3'	5'ACGTAGTAGACGATGGGCAG3'
Wnt5a	Wnt family member 5a	5' CAACTGGCAGGACTTTCTCAA 3'	5'CCTGATACAAGTGGCAGAGTTT3'
Wnt10b	Wnt Family Member 10b	5'CCAGGTGGTAACGGAAAACC3'	5'TGCCCTCCAACAGGTCTTG3'
Gapdh	Glyceraldehyde-3-phosphate dehydrogenase	5'TCAGCAATGCCTCCTGCAC3'	5'TCTGGGTGGCAGTGATGGC3'
Actb	Actin, beta	5'ACTGAGCGTGGCTATTCCTTCG3'	5'CTAGGGCCGTGATCTCCTTCTG3'

Table 2. Primer sequences for the genes investigated in this study (rat)

Gene	Full name	Forward sequences	Reverse sequences
Runx2	Runx family transcription factor 2	5'AAATGCCTCCGCTGTTATGAA3'	5'GCTCCGGCCCACAAATCT3'
OCN	Bone gamma-carboxyglutamate protein	5'CCGGGAGCAGTGTGAGCTTA3'	5'AGGCGGTCTTCAAGCCATACT3'
OPN	Secreted phosphoprotein 1	5'CGCTCGTGTTTCTGGACATCT3'	5'CACACGGTCTTCCACTTTGC3'
ALP	Alkaline phosphatase, biomineralization associated	5'AGGGTGGGTAGTCATTTGCATAG3'	5'GAGGCATACGCCATCACATG3'
Smad1	Smad family member 1	5'GTATGAGCTTTGTGAAGGGC3'	5'TAAGAACTTTATCCAGCCACTGG3'
Smad4	Smad family member 4	5'CTCCAGCTATCAGTCTGTCAG3'	5'CCCGGTGTAAGTGAATTTCAAT3'
Smad5	Smad family member 5	5'TCATCATGGCTTTCATCCCACC3'	5'GCTCCCCAACCCTTGACAAA3'

| BMPR2	Bone morphogenetic protein receptor type 2	5'GCTCCACAAACGAGAAAAGC3'	5'AGCAAGGGGAAAAGGACACT3'
VEGFA	Vascular endothelial growth factor A	5'GTCCCATGAAGTGATCAAGTTC3'	5'TCTGCATGGTGATGTTGCTCTCTG3'
VEGFR	Vascular endothelial growth factor receptor	5'GAGAACACCAGAGTATGCCACACCT3'	5'TCAAAACAGCGACAACAAACAAAAC3'
ATG5	Autophagy related 5	5'GCTCTGCCTTGGAACATCAC3'	5'GAGTTTCCGGTTGATGGTCC3'
ATG7	Autophagy related 7	5'GTCAGCCAATGAGATCTGGG3'	5'TCATCGTAGGCATGCTCCAG3'
Beclin 1	Beclin 1	5'TGGACCGAGTGACCA TTCAG3'	5'GGGTGATCCACATCTGTCTG3'
Actb	Actin, beta	5'ATGCAGCCTGAAGAGGACTG3'	5'GGCTATGAAATCCAGGGCCT3'

Figure legends
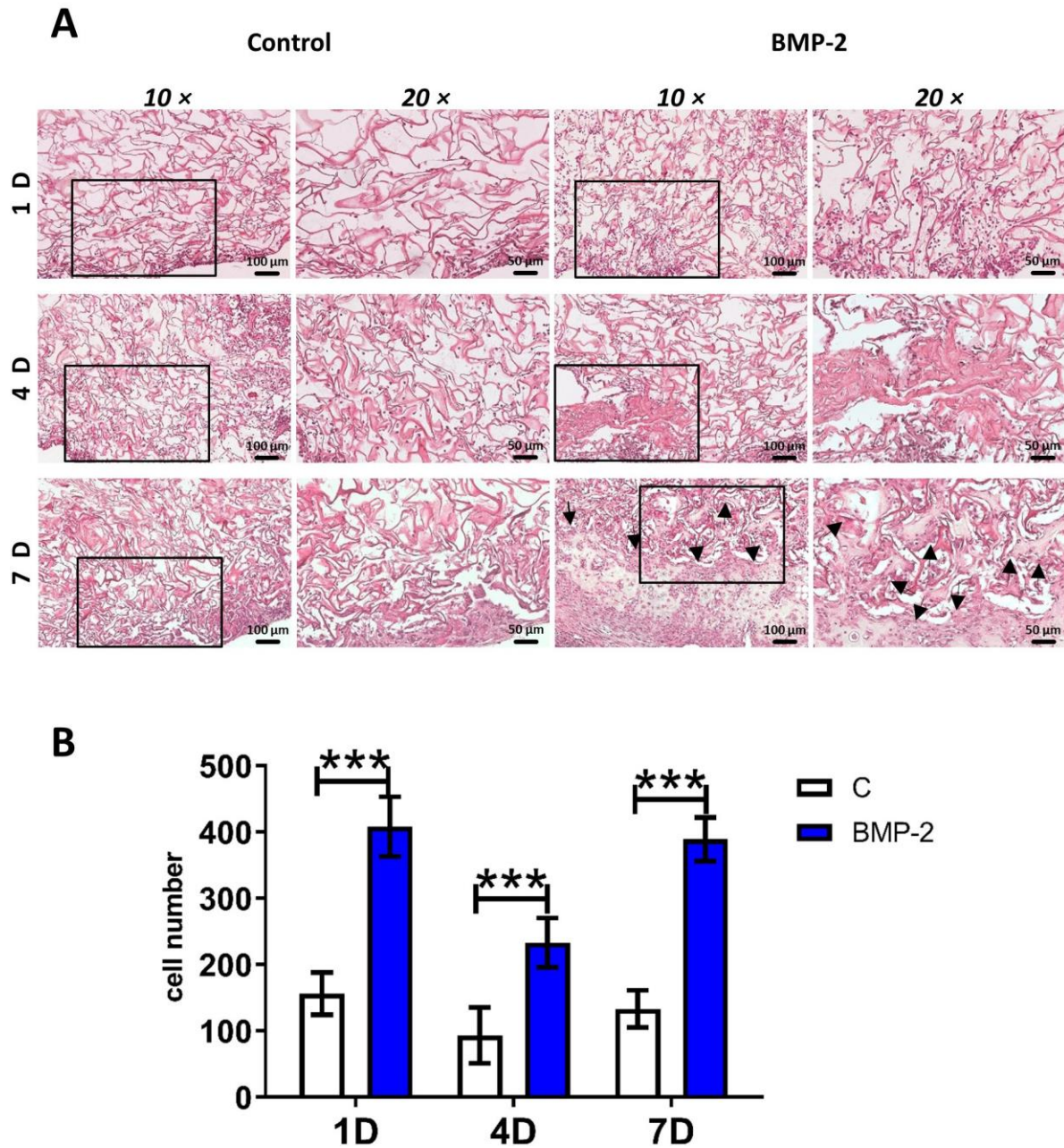
Figure 1. Histology observation of subcutaneous osteogenic (BMP-2 application) model. (A) Representative images of histologic (original magnification, 100×, 200×) observations of subcutaneous tissues from the control and BMP-2 groups. At 7 days after implantation, bone-like structures could only be observed in BMP-2 group (as indicated by arrows). Compared with the control group, more cells infiltrated into the subcutaneous tissues of BMP-2 group, the morphology of which suggested that they generally consisted of fibroblast-like cells and infiltrating immune cells. (B) Measurements of total cell numbers
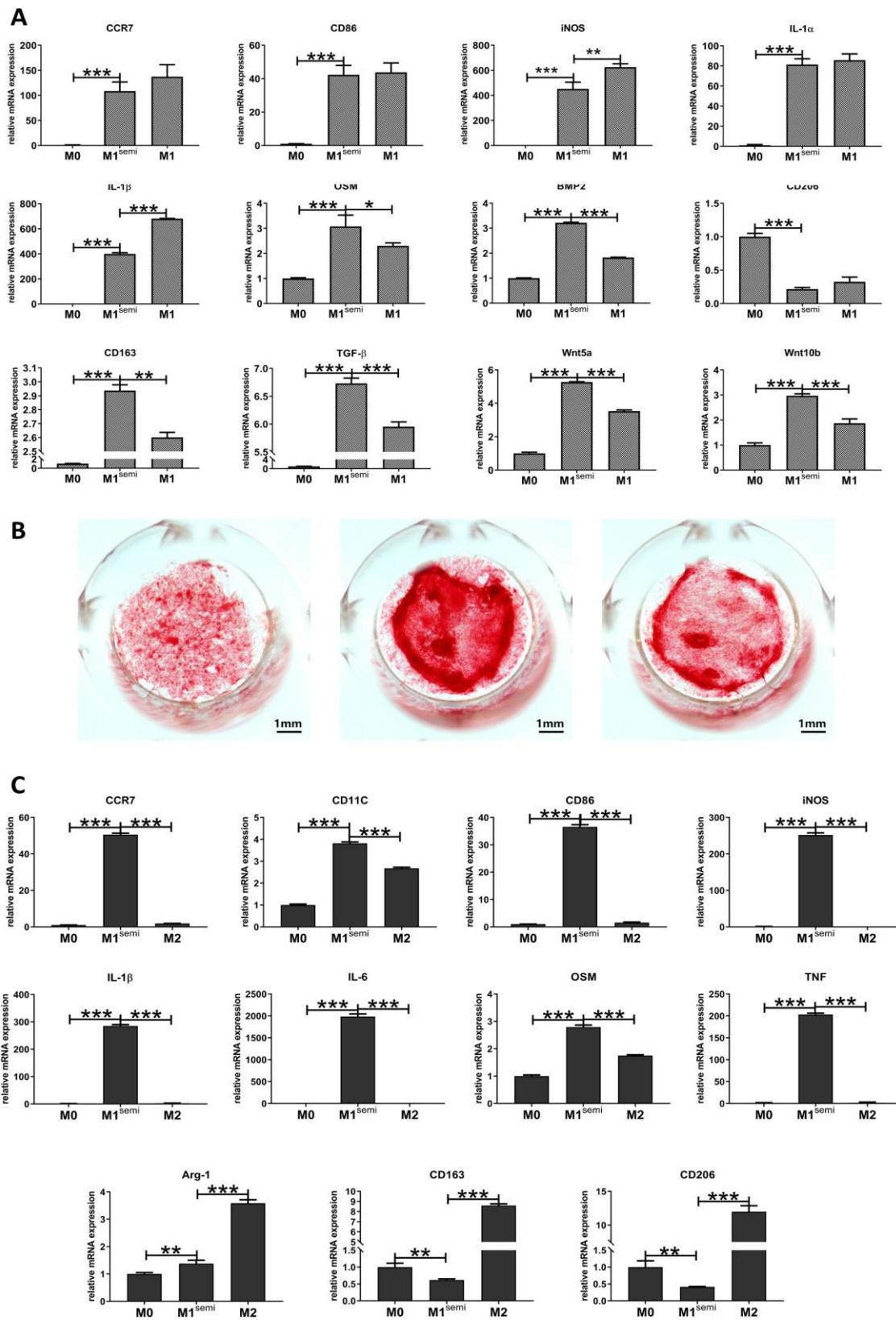
in tissues from control and BMP-2 groups. Significant differences were observed (***$P <$ 0.001). C = control group, BMP-2 = BMP-2 group, 1/4/7 D: 1/4/7 days after implantation. For cell-counting, we measured the number of cells from each image generated from tissue sections (5 areas were randomly chosen). The average number of the 5 measurements from each section was calculated as the mean value. Three sections were used from each animal sample. For statistical analysis, therefore, there were 9 data collected from each group (3 slices * 3 animals).
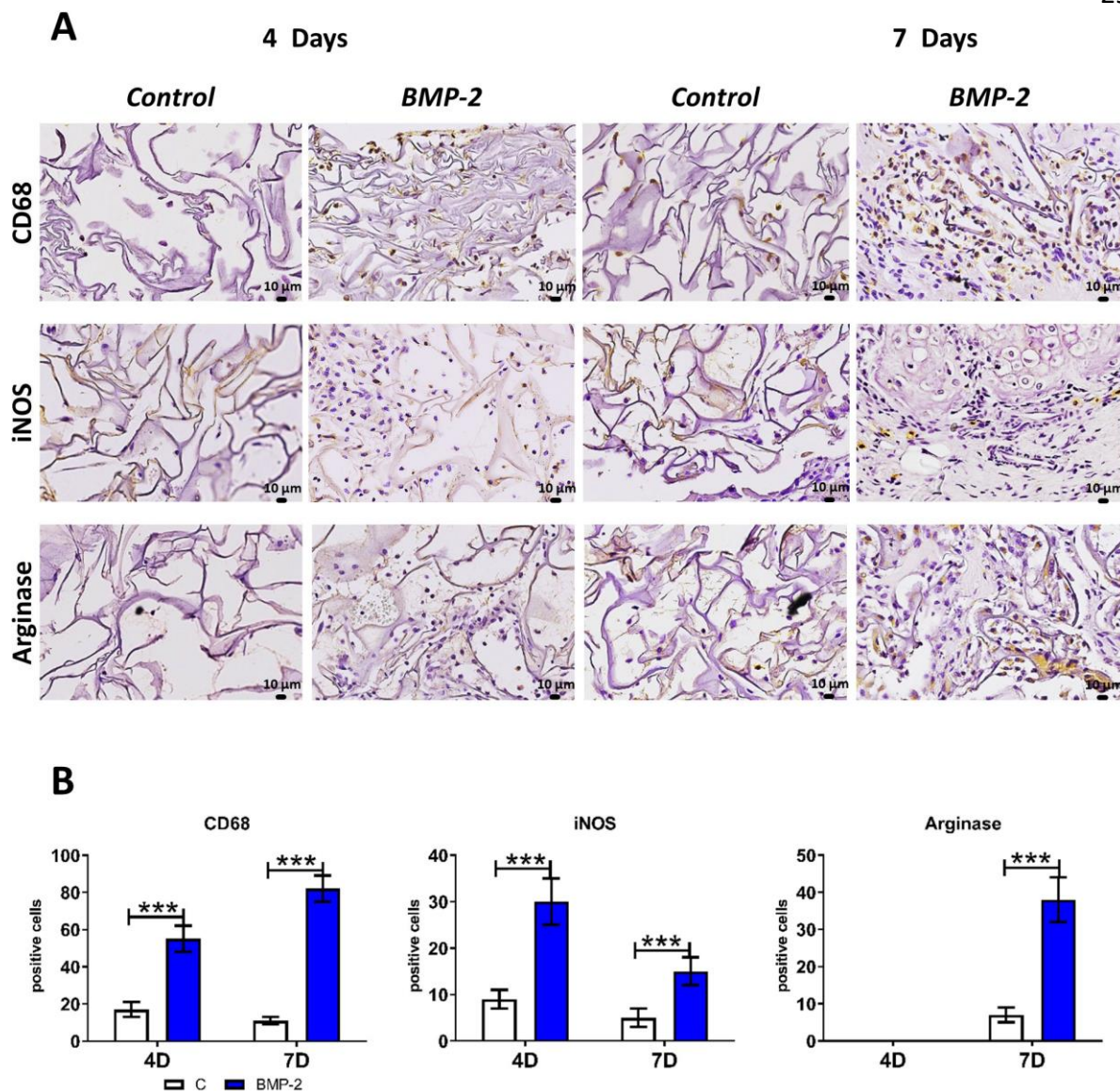
Figure 2. Macrophage infiltration/polarization in the subcutaneous osteogenic model. (A) Representative images of IHC (original magnification, 400×) observations of subcutaneous tissues from the control and BMP-2 groups. Compared with the control group, CD68 and iNOS expression was enhanced in BMP-2 group at 4 and 7 days after implantation. Arginase expression was also induced in BMP-2 group at day 7. In BMP-2 group, CD68 and arginase expression kept increasing from day 4 to day 7, while iNOS expression peaked at day 4 then decreased thereafter. (B) Measurements of CD68+, iNOS+ and arginase+ cells in subcutaneous from the two groups. Significant differences were observed (***P < 0.001). C = control group, BMP-2 = BMP-2 group, 4/7 D: 4/7 days after implantation.
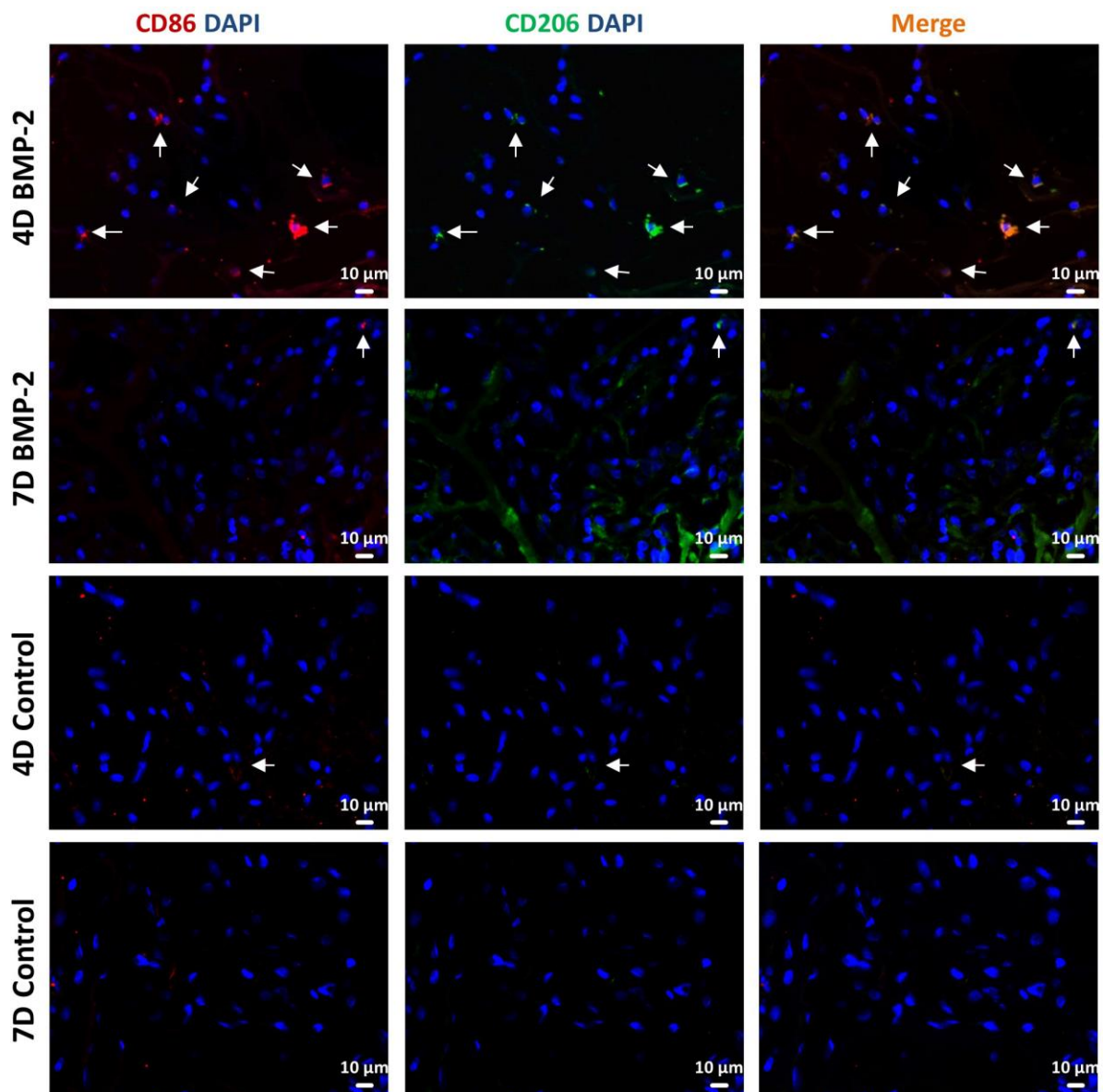
Figure 3. Double-immunofluorescent (IF) staining to identify cells expressing both M1 (CD86) and M2 (CD206) markers. CD86$^+$ cells (red) and CD206$^+$ cells (green) cells in day 4/day7 samples from control and BMP-2 groups were detected. Arrows point to the cells expressing both CD86 and CD 206 (brown color in the merged image). Blue color: DAPI staining for nuclei. Control = control group, BMP-2 = BMP-2 group, 4/7D: 4/7 days after implantation.

Figure 4. Comparison of semi-activated macrophage (M1^{semi}) and typical M0/M1/M2 macrophage phenotypes. (A) The mRNA levels (original data were normalized against M0

group and appeared as fold changes) of inflammatory genes (*CCR7, CD86, iNOS, IL-1α/β*) were significantly induced in both M1^{semi} and M1 macrophages, however, M1^{semi} group) showed reduced expression of inflammatory markers (*iNOS* and *IL-1β*) while induced anti-inflammatory/osteogenic markers (*OSM*, *BMP2, CD206, CD163, TGF-β, Wnt5a* and *Wnt10b*. Significant differences were observed (*P < 0.05, ** *P* < 0.01, ***P < 0.001). M0/M1^{semi}/M1 = M0/M1^{semi}/M1 macrophages. (B) Alizarin Red staining result of rBMSCs applied with CM from M0, M1^{semi} and M1 macrophages during osteogenic differentiation for 14 days. M1^{semi} CM treated cells showed induced positive stain. M0/M1^{semi}/M1 = rBMSCs treated with CM from M0/M1^{semi}/M1 macrophages. (C) Represented mRNA levels of M1-like inflammatory (*CCR7, CD11C, CD86, iNOS, IL-1β, IL-6* and *TNF*), osteoinductiove (OSM) and anti-inflammatory markers (*Arg-1, CD163, CD206*) in M0, M1semi and M2 macrophages. Data from each group were normalized to the M0 group and appeared as fold changes. Data are presented as the mean ± SD (n = 3). *P < 0.05, **P < 0.01, ***P < 0.001). M0/M1semi/M2 = M0/M1semi/M2 macrophages.
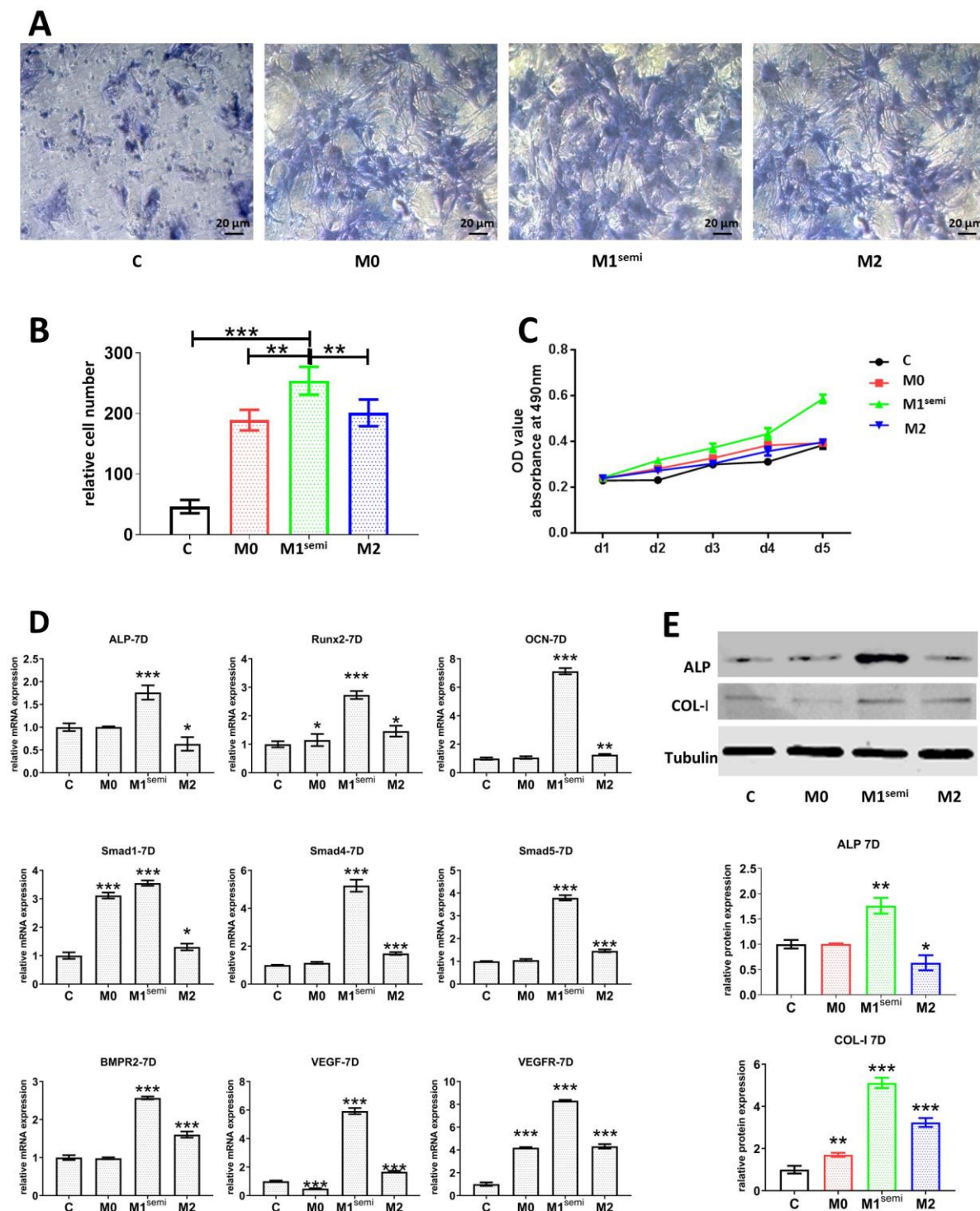
Figure 5. M1^semi CM induced migration, proliferation, and osteogenic differentiation in rBMSCs. (A) Transwell assay result showed that there more cells attracted by M1^semi CM (original magnification, 200×), as compared with the control group and the M0 and M2 CM treated cells. (B) Cell migration quantification of the control, M0, M1^semi and M2 groups. Data were normalized against the control group (100 %). Significant differences were

observed (** $P < 0.01$, ***$P < 0.001$). (C) The effects of M0, M1^{semi} and M2 CM on cell metabolism were examined by MTT assay. M1^{semi} CM treated cells showed enhanced metabolism level, suggesting cell proliferation should be improved in M1^{semi} group. (D) The mRNA levels (original data were normalized against the control group and appeared as fold changes) of osteogenesis-related factors (*ALP, Runx2, OCN, Smad 1/4/5, BMPR2, VEGF and VEGFR*) were examined. M1^{semi} CM treated cells showed the highest levels of these markers (*$P < 0.05$, ** $P < 0.01$, ***$P < 0.001$). (E) Protein levels of osteogenic markers (ALP and COL-I) were significantly induced in M1^{semi} CM treated cells (*$P < 0.05$, ** $P < 0.01$, ***$P < 0.001$). M0/M1^{semi}/M2 = rBMSCs treated with CM from M0/M1^{semi}/M2 macrophages, C = control group, 3 D = 3 days of differentiation, 7 D = 7 days of differentiation.
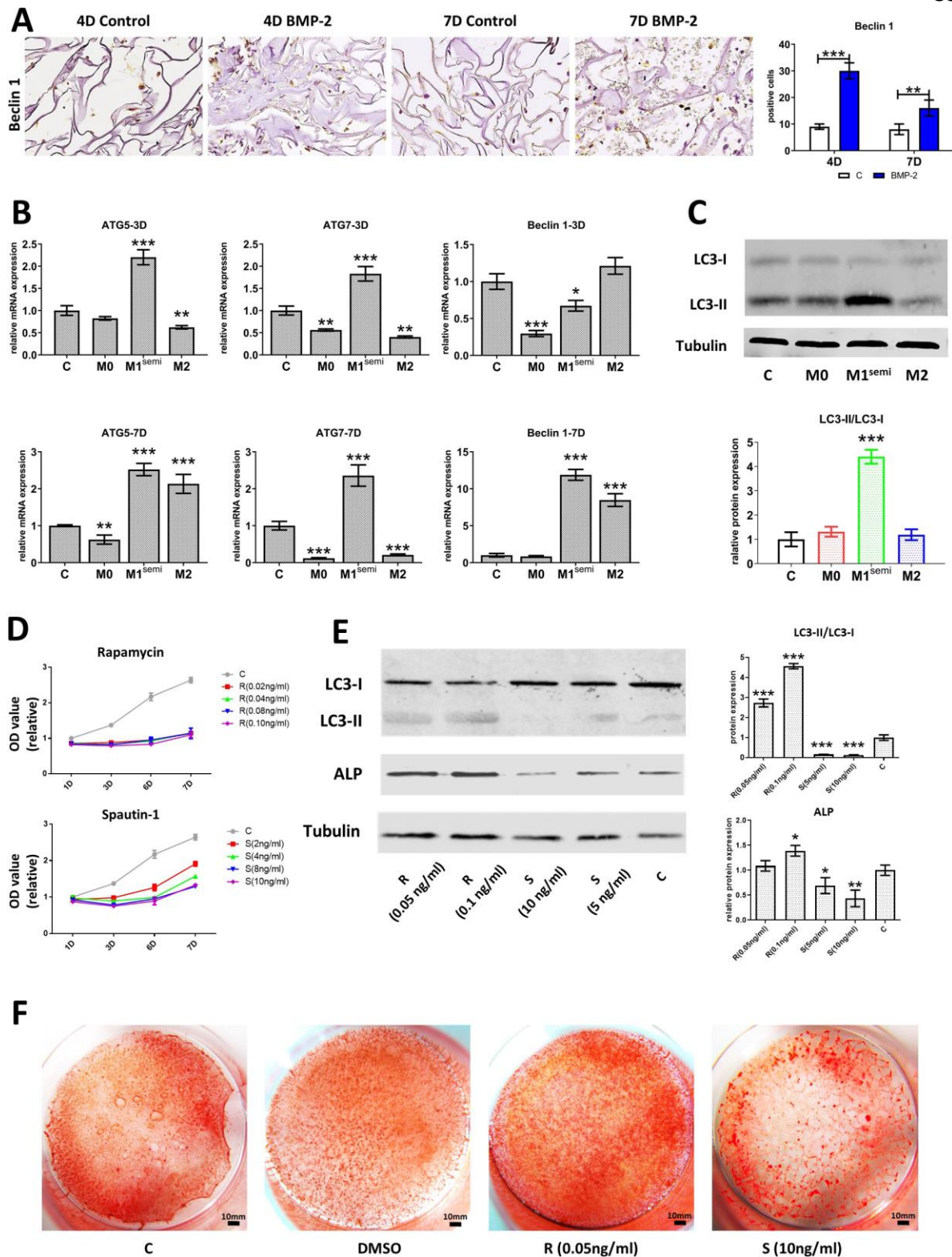
Figure 6. Involvement of autophagy in macrophage-BMSC interaction during osteogenesis. (A) Representative images of IHC (original magnification, 400×) observations of beclin 1 in subcutaneous tissues from the control and BMP-2 groups. Compared with the control

group, the expression of beclin 1 was significantly induced, which peaked at 4 days after implantation, as indicated by the measurement data. C = control group, BMP-2 = BMP-2 group, 4/7 D: 4/7 days after implantation. (B) The mRNA levels (original data were normalized against the control group and appeared as fold changes) of autophagy-related genes (*ATG5, ATG7, beclin 1*) were examined in rBMSCs during osteogenesis, and the M1^{semi} CM treated cells showed the highest levels of these markers. M0/M1^{semi}/M2 = rBMSCs treated with CM from M0/M1^{semi}/M2 macrophages. C = control group. (C) Protein levels suggested that LC3-I to LC3-II turnover was significantly induced in M1^{semi} CM treated cells. M0/M1^{semi}/M2 = rBMSCs treated with CM from M0/M1^{semi}/M2 macrophages. C = control group. (D) MTT assay results of rBMSCs treated with spautin-1 and rapamycin at graded doses (original data were normalized against the control group on day 1). (E) Protein levels suggested that spautin-1/rapamycin decreased/increased LC3-I to LC3-II turnover in a dose-dependent manner in rBMSCs with osteogenic differentiation, respectively, which was inconsistence with ALP expression change. C = control group, R= rBMSCs treated with rapamycin, S = rBMSCs treated with spautin-1. (F) Alizarin Red staining result suggested that cell mineralization was induced/reduced following rapamycin/spautin-1 treatments, respectively (cells treated with DMSO served as the vehicle control). C = control group, DMSO = vehicle control, R= rBMSCs treated with rapamycin, S = rBMSCs treated with spautin-1, 3 D = 3 days of differentiation, 7 D = 7 days of differentiation. *$P < 0.05$, ** $P < 0.01$, ***$P < 0.001$.
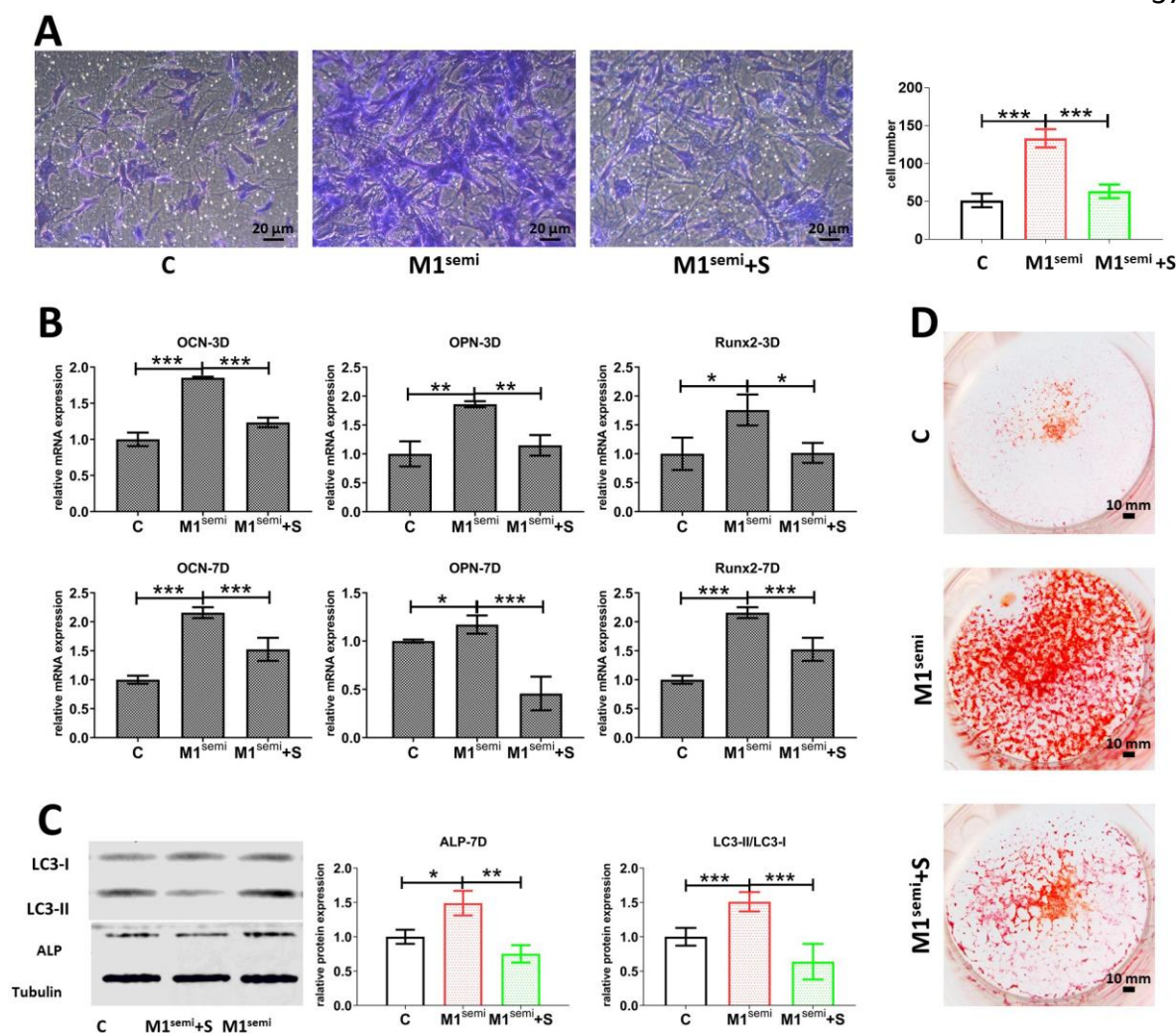
Figure 7. M1^semi macrophage promoted migration and osteogenesis in an autophagy-dependent manner. (A) Transwell assay result showed that the induced cell migration (original magnification, 200×) diminished when applied with autophagy inhibitor spautin-1, as indicated by the quantitative data. (B) The increased mRNA levels (original data were normalized against the control group and appeared as fold changes) of osteogenic markers (OCN, OPN and Runx2) by M1^semi CM were reduced in rBMSCs with autophagy inhibitor spautin-1. (C) ALP protein level and LC3-I to LC3-II turnover were reduced in M1^semi CM treated cells following autophagy inhibition. (D) Alizarin red staining suggested that mineralization of rBMSCs was downregulated in M1^semi CM treated cells following autophagy inhibition. *$P < 0.05$, ** $P < 0.01$, ***$P < 0.001$. C = control group, M1^semi = rBMSCs treated with CM from M1semi macrophages, M1^semi + S = rBMSCs treated with M1semi CM and spautin-1, 3 D = 3 days of differentiation, 7 D = 7 days of differentiation.